Assessment of Treatment Response in Patients with Glioblastoma Using *O*-(2-^{18}F-Fluoroethyl)-L-Tyrosine PET in Comparison to MRI

Norbert Galldiks[1,2], Karl-Josef Langen[1,3], Richard Holy[3,4], Michael Pinkawa[3,4], Gabriele Stoffels[1,3], Kay W. Nolte[3,5], Hans J. Kaiser[3,6], Christan P. Filss[1,3], Gereon R. Fink[1,2], Heinz H. Coenen[1,3], Michael J. Eble[3,4], and Marc D. Piroth[3,4]

[1]*Institute of Neuroscience and Medicine, Forschungszentrum Jülich, Jülich, Germany;* [2]*Department of Neurology, University Hospital Cologne, Cologne, Germany;* [3]*Section JARA-Brain, Jülich-Aachen Research Alliance (JARA), Jülich, Germany;* [4]*Department of Radiation Oncology, RWTH Aachen University Hospital, Aachen, Germany;* [5]*Institute of Neuropathology, RWTH Aachen University Hospital, Aachen, Germany; and* [6]*Department of Nuclear Medicine, RWTH Aachen University Hospital, Aachen, Germany*

The assessment of treatment response in glioblastoma is difficult with MRI because reactive blood–brain barrier alterations with contrast enhancement can mimic tumor progression. In this study, we investigated the predictive value of PET using *O*-(2-^{18}F-fluoroethyl)-L-tyrosine (^{18}F-FET PET) during treatment. **Methods:** In a prospective study, 25 patients with glioblastoma were investigated by MRI and ^{18}F-FET PET after surgery (MRI-/FET-1), early (7–10 d) after completion of radiochemotherapy with temozolomide (RCX) (MRI-/FET-2), and 6–8 wk later (MRI-/FET-3). Maximum and mean tumor-to-brain ratios (TBR_{max} and TBR_{mean}, respectively) were determined by region-of-interest analyses. Furthermore, gadolinium contrast-enhancement volumes on MRI (Gd-volume) and tumor volumes in ^{18}F-FET PET images with a tumor-to-brain ratio greater than 1.6 ($T_{vol\ 1.6}$) were calculated using threshold-based volume-of-interest analyses. The patients were grouped into responders and nonresponders according to the changes of these parameters at different cutoffs, and the influence on progression-free survival and overall survival was tested using univariate and multivariate survival analyses and by receiver-operating-characteristic analyses. **Results:** Early after completion of RCX, a decrease of both TBR_{max} and TBR_{mean} was a highly significant and independent statistical predictor for progression-free survival and overall survival. Receiver-operating-characteristic analysis showed that a decrease of the TBR_{max} between FET-1 and FET-2 of more than 20% predicted poor survival, with a sensitivity of 83% and a specificity of 67% (area under the curve, 0.75). Six to eight weeks later, the predictive value of TBR_{max} and TBR_{mean} was less significant, but an association between a decrease of $T_{vol\ 1.6}$ and PFS was noted. In contrast, Gd-volume changes had no significant predictive value for survival. **Conclusion:** In contrast to Gd-volumes on MRI, changes in ^{18}F-FET PET may be a valuable parameter to assess treatment response in glioblastoma and to predict survival time.

Despite all efforts to improve treatment strategies, the prognosis of patients with glioblastoma to date remains poor (*1*). Standard therapy includes surgery and radiotherapy with concomitant and adjuvant temozolomide chemotherapy (*2*). MRI is the most important diagnostic tool for assessing brain neoplasms, and in malignant gliomas (*3*) the extent of contrast enhancement on MRI is used as an indicator of therapeutic response although the reliability in distinguishing tumor tissue from unspecific treatment effects such as postsurgery blood–brain barrier breakdown is limited (*4*). For example, reactive transient blood–brain barrier alterations with consecutive contrast enhancement can mimic tumor progression. This phenomenon, so-called pseudoprogression, is seen in 20%–30% of cases (*5*) and may result in an unnecessary overtreatment. Consequently, alternative diagnostic methods are needed to improve the assessment of treatment response (*6*).

The rationale for using radiolabeled amino acids such as *O*-(2-^{18}F-fluoroethyl)-L-tyrosine (^{18}F-FET) to measure treatment response in cerebral gliomas is based on high uptake of the radiotracer in these tumors—uptake that is likely to reflect an increased expression of amino acid transporters (*7*). Amino acid uptake in gliomas is independent of blood–brain barrier disruption, and increased ^{18}F-FET uptake has also been observed in nonenhancing tumor areas that are difficult to delineate using MRI (*8*). Furthermore, contrast-enhancing nontumoral tissue on MRI, for example, due to radionecrosis, is usually negative on ^{18}F-FET PET (*9*). Thus, ^{18}F-FET PET may be a promising tool to improve the evaluation of treatment response.

Current experience with radiolabeled amino acids concerning treatment monitoring and prediction of outcome is promising (*10–15*), but the parameters derived from amino acid PET to assess treatment response vary among different studies. Some studies suggested that a change of the maximal tumor-to-brain ratio (TBR) may be the most reliable parameter for the identification of tumor progression (*9*), whereas other studies suggest that changes in the tumor volume delineated by amino acid PET may be more sensitive than standardized uptake values (*16*).

This prospective study systematically evaluated the time course of different parameters derived from ^{18}F-FET PET during treatment of glioblastoma in comparison to conventional MRI for assessing treatment response with respect to survival time of the patients. A preliminary evaluation of the data indicated that ^{18}F-FET PET was indeed helpful at predicting treatment response and outcome of the patients at an early stage of the disease (*17*). In this final evaluation, the ultimate size of the patient population and a longer follow-up period are considered. In addition, various parameters derived from ^{18}F-FET PET and the examination of tumor volume on MRI are included in the analysis.

MATERIALS AND METHODS

Patients

From January 2007 to June 2010, a group of 25 consecutive patients with glioblastoma were included in this prospective study. There were 15 men and 10 women; the mean age was 54 y (range, 36–73 y). The tumor was located in the frontal, temporal, parietal, and occipital lobes in 9, 7, 8, and 1 patients, respectively. All patients were treated with cytoreductive surgery. According to neurosurgical reports, 13 surgical interventions were rated as partial resections and 12 as gross total resections, although considerable tumor remnants were detected on ^{18}F-FET PET in most of these patients (Table 1). Surgery was followed by an external fractionated radiotherapy with concomitant temozolomide (RCX; 75 mg of temozolomide per square meter of body surface area per day, 7 d per week from the first to the last day of radiotherapy) and, after a 4-wk break, by adjuvant temozolomide chemotherapy (150–200 mg of temozolomide per square meter of body surface area over 5 d, repeated every 23 d, 6 cycles) according to EORTC trial 22981/26981 (*2*). During adjuvant temozolomide therapy, patients underwent a monthly clinical evaluation, and after completion of adjuvant temozolomide therapy a clinical evaluation was performed every 2–3 mo.

The general prognosis of the patients was classified by the commonly used recursive partitioning analysis (RPA) scores including a set of pretreatment- and treatment-related prognostic variables (*18*). O[6]-methylguanine-DNA methyltransferase status (MGMT) could be determined in 22 patients (*19*). Further details on the patient group are given in Tables 1 and 2. The university ethics committee and federal authorities approved this study. All subjects gave written informed consent before their participation in the study.

Radiotherapy

In all patients, a total dose of 60 Gy was administered to the planning target volume 1 (PTV1), defined as the contrast-enhanced area from pre- and postoperative MRI including a safety margin of 2–3 cm and including the surrounding preoperative edema. The dose was prescribed to the reference point of the International Commission on Radiation Units and Measurements (*20*), and the fractionation was 2 Gy daily, 5 times weekly. Radiation treatment was planned in 5 of the 25 patients with the standard 3-dimensional radiation treatment. The remaining 20 patients underwent intensity-modulated radiotherapy. In these patients, an additional planning target volume (PTV2) was created and defined as the ^{18}F-FET–positive tumor volume within a cutoff of 1.6 or more for the TBR of ^{18}F-FET uptake. In all patients, the pathologic ^{18}F-FET volume PTV2 was covered by the PTV1. The total dose for PTV2 was 72 Gy, and the mean dose for the larger PTV1 was 60 Gy, as in the other patients. The Pinnacle irradiation treatment planning system (version 8.0m; Philips) was used for radiation treatment planning.

MRI and Analysis

All patients underwent routine MRI using a 1.5-T scanner with a standard head coil before and after administration of gadolinium–diethylenetriaminepentaacetic acid (T1, T2, and fluid-attenuated inversion recovery sequences; slice thickness, 1 mm). The first MRI scan (MRI-1) was obtained within 11–20 d after surgery, the second MRI scan (MRI-2) 7–10 d after completion of RCX, and the third MRI scan (MRI-3) 6–8 wk after completion of RCX. After MRI-3, a follow-up MRI scan was obtained every 8–12 wk. As previously described (*21*), in all patients gadolinium contrast–enhancing volumes on MRI (Gd-volume) were measured by performing a 3-dimensional threshold-based volume-of-interest analysis using the VINCI tool (*22*). The threshold for contrast enhancement on MRI was determined by varying the value of the lower threshold to identify and separate the area of contrast enhancement from the tissue with lower intensity (*21*).

PET with ^{18}F-FET and Analysis

The amino acid ^{18}F-FET was produced via nucleophilic ^{18}F-fluorination with a specific radioactivity of greater than 200 GBq/μmol, as described previously (*23*). All patients fasted for at least 12 h before the PET studies. Dynamic PET studies were performed up to 50 min after intravenous injection of 200 MBq of ^{18}F-FET on an ECAT EXACT HR+ scanner (Siemens Medical Systems, Inc.) in 3-dimensional mode (32 rings; axial field of view, 15.5 cm). Further evaluation was based on the summed ^{18}F-FET PET data from 20 to 40 min after injection. Attenuation correction and data reconstruction were performed as described previously (*8*). The PET studies were done in temporal correspondence to MRI.

^{18}F-FET PET and MRI were automatically coregistered using the VINCI tool (*22*). The fusion results were inspected and, if necessary, adapted using anatomic landmarks. ^{18}F-FET uptake in the unaffected brain tissue was determined by a larger region of interest (ROI) placed on the contralateral hemisphere in an area of normal-appearing brain tissue including white and gray matter (mean area, $2,082 \pm 369$ mm^2). The tumor area on ^{18}F-FET PET scans was determined by a 3-dimensional autocontouring process using a cutoff of 1.6 or more for the TBR of ^{18}F-FET uptake. This cutoff was based on a previous biopsy-controlled study in which a lesion-to-brain ratio of 1.6 had best separated tumor from nontumor tissue (*8*). Manual corrections of the tumor ROI were applied if the radioactivity in blood vessels or tracer uptake in postoperative extracerebral soft tissue exceeded the cutoff value. Maximum and mean TBR (TBR_{max} and TBR_{mean}, respectively) were calculated by dividing the mean and maximum ROI

TABLE 1
Patient Characteristics, TBR_{max}, TBR_{mean}, and $T_{vol\ 1.6}$ in ^{18}F-FET PET, Gd-Volumes in MRI, PFS, and OS

Patient no.	Age (y)	Sex	OP	FET-/MRI-1 TBR_{max}	TBR_{mean}	$T_{vol\ 1.6}$ (cm³)	Gd-volume (cm³)	FET-/MRI-2 TBR_{max}	TBR_{mean}	$T_{vol\ 1.6}$ (cm³)	Gd-volume (cm³)	FET-/MRI-3 TBR_{max}	TBR_{mean}	$T_{vol\ 1.6}$ (cm³)	Gd-volume (cm³)	PFS (mo)	OS (mo)
1	59	F	T	2.6	1.8	1.6	0.9	NA	NA	NA	4.3	2.1	1.6	2.4	5.4	14.1	16.1
2	47	M	P	4.1	2.1	61.9	14.2	4.0	3.2	97.0	22.0	3.5	2.0	98.1	26.0	8.3	9.3
3	62	F	P	3.5	2.0	54.8	NA	4.6	2.3	81.7	14.8	4.3	2.3	79.2	23.1	5.1	5.6
4	51	M	T	3.6	2.1	8.1	6.0	2.8	1.9	13.6	3.7	3.1	2.1	7.0	1.7	9.4	22.8
5	60	M	P	4.1	2.3	74.3	31.6	3.4	2.3	40.1	5.2	3.6	2.6	50.2	28.4	5.4	6.9
6	58	M	T	3.6	2.2	7.7	0.6	3.0	2.0	10.9	2.7	2.8	2.0	11.6	3.2	7.2	28.5
7	50	M	P	4.6	2.4	16.0	6.1	3.2	2.0	6.2	0.5	2.3	1.8	12.0	0.6	19.3	28.5
8	45	F	T	2.0	1.7	0.3	0.0	1.7	1.6	0.7	0.0	2.0	1.7	0.4	0.0	13.9	14.8
9	36	M	P	2.3	1.9	15.3	1.3	3.2	2.2	28.0	6.4	3.5	2.0	31.2	14.8	4.7	9.3
10	51	M	P	3.7	2.5	9.1	1.1	2.3	1.7	1.3	0.6	3.1	1.9	5.4	1.2	5.3	16.1
11	61	F	P	3.3	2.2	35.9	16.8	3.3	2.2	27.9	8.7	*	*	*	*	2.8	2.8
12	58	M	T	2.2	1.7	2.3	1.6	1.5	1.2	0.3	0.9	2.0	1.7	1.3	0.3	28.7†	28.7‡
13	71	M	T	2.0	1.7	1.0	5.2	2.1	1.8	1.5	NA	2.0	1.8	1.0	NA	5.5	8.5
14	54	M	T	4.9	2.6	64.0	19.4	2.8	1.9	37.5	2.3	3.2	1.9	37.3	4.5	5.2	10.5
15	62	F	P	3.6	2.1	10.3	6.8	2.5	1.8	5.9	NA	2.6	2.0	7.2	5.6	10.3	14.8
16	48	F	P	4.8	2.9	45.5	19.5	3.8	2.9	30.0	3.9	2.7	3.1	61.1	36.3	3.3	14.3
17	73	F	P	3.3	2.0	3.6	8.2	2.6	1.9	3.4	0.4	2.4	2.0	7.0	0.2	12.9	15.4
18	50	M	P	3.1	2.0	8.8	0.8	2.5	2.0	15.6	6.2	2.0	1.7	1.4	3.2	7.8	9.8
19	64	M	T	3.8	2.2	19.9	1.3	2.4	1.8	6.7	6.9	2.5	1.9	9.8	6.1	9.3	20.9
20	53	M	T	3.1	2.1	7.0	2.2	2.5	1.9	5.7	0.6	2.5	1.8	3.7	NA	6.6	8.2
21	55	F	P	2.9	2.0	8.2	4.9	2.6	1.9	12.8	4.6	2.5	1.9	11.0	12.5	5.8	9.9
22	58	F	P	2.4	1.8	6.9	3.7	2.8	2.0	9.0	2.8	3.7	2.5	11.4	2.9	3.8	13.8
23	39	F	T	2.4	1.9	15.0	0.1	2.0	1.7	1.0	1.8	2.0	1.7	1.4	1.0	15.7†	15.7‡
24	47	M	T	2.5	2.0	4.7	6.5	NA	NA	NA	NA	2.4	1.9	10.6	35.1	5.2	6.8
25	50	M	T	2.0	1.6	0.4	6.4	1.4	1.1	0.1	0.0	2.0	1.7	0.1	0.0	13.3	13.3‡

*Patient died.
†Censored for PFS; patient without recurrence of glioblastoma.
‡Censored for OS; patient alive.
OP = resection status according to neurosurgical report; T = total resection; NA = not available; P = partial resection.

TABLE 2
Univariate Survival Analysis of General Prognostic Factors

Factor	n	%	PFS (mo) Value	P	Hazard ratio	95% confidence interval	OS (mo) Value	P	Hazard ratio	95% confidence interval
RPA score				0.08	0.393	0.132–1.164		0.30	0.682	0.247–1.884
III/IV	20	80	8.3				14.3			
V/VI	5	20	5.4				8.5			
Extent of resection				0.06	0.502	0.221–1.139		0.06	0.554	0.244–1.260
Gross total resection	12	48	9.3				16.1			
Partial resection	13	52	5.4				9.9			
$T_{vol\ 1.6}$ in FET-1				0.002*	0.213	0.073–0.617		0.001*	0.215	0.073–0.633
$<25\ cm^3$	19	76	9.3				15.4			
$>25\ cm^3$	6	24	5.1				6.9			
MGMT status				0.03*	0.264	0.086–0.816		0.008*	0.172	0.048–0.615
Positive	6	24	12.9				20.9			
Negative	16	64	5.5				9.9			
Not known	3	12								
Prescribed dose				0.63	1.377	0.505–3.756		0.71	0.933	0.344–2.529
60 Gy (PTV1)	5	20	8.3				9.3			
60 Gy (PTV1)/72 Gy (PTV2)	20	80	7.2				14.3			

*Significant.
RPA score = recursive partitioning analysis of prognostic factors; MGMT status = O^6-methylguaninemethyltransferase status.

value (Bq/mL) of the tumor lesion by the mean ROI value of normal brain tissue in the ^{18}F-FET PET scans. The ^{18}F-FET–positive tumor volume at a cutoff of 1.6 or more for the TBR ($T_{vol\ 1.6}$) was determined.

Definition of Pseudoprogression

Usually, contrast enhancement on MRI during pseudoprogression occurs within the first 8 wk after completion of RCX and invariably undergoes spontaneous clinical and radiographic improvement without intervention (6). Accordingly, in our study we identified patients with an increase of the Gd-volume of more than 50% between MRI-1 and MRI-3, followed by subsequent regression of contrast enhancement on follow-up MRI scans.

Definition of Survival Times

Overall survival (OS) time was defined as the interval from date of surgery to date of death or, if the patients were still alive, as the interval from date of surgery to date of last contact. Progression-free survival (PFS) was defined as the interval from date of surgery to date of first documented evidence of disease progression, based on decline shown by the MR image or neurologic deterioration. Progressive disease on the MR image was defined according to the criteria of Macdonald et al. (24).

Assessment of Treatment Effects on Prognosis

The relative and absolute changes of TBR_{max}, TBR_{mean}, $T_{vol\ 1.6}$, and Gd-volumes at the second diagnostic scan (MRI and ^{18}F-FET PET early [7–10 d] after completion of radiochemotherapy with temozolomide [RCX] [MRI-2 and FET-2, respectively]) and at the third diagnostic scan (MRI and ^{18}F-FET PET 6–8 wk later [MRI-3 and FET-3, respectively]) after completion of RCX were determined in relation to baseline imaging (MRI and ^{18}F-FET PET after surgery [MRI-1 and FET-1, respectively]). To analyze the prognostic value of changes of TBR_{max}, TBR_{mean}, metabolically

active tumor volumes ($T_{vol\ 1.6}$), and Gd-volumes in serial ^{18}F-FET PET and MRI on OS and PFS, patients were subdivided into responders and nonresponders according to the changes of the different imaging parameters. In an approximation process, different cut points of the various parameters were used to determine the value best separating the patients into 2 prognostic groups (Table 3; Supplemental Tables 1–4 [supplemental materials are available online only at http://jnm.snmjournals.org]). The diagnostic value of the various parameters for the prediction of treatment success was also tested using a receiver-operating-characteristic (ROC) analysis. Therefore, the patient population was divided into a partition with longer survival (PFS/OS > median) and a partition with shorter survival (PFS/OS < median). Along with the ROC analysis, the extent to which the individual parameters identified those patients with shorter survival was examined (Supplemental Table 1).

On the basis of our experiences with other tyrosine derivates, we assumed only a change of greater than 5% of the TBR of ^{18}F-FET uptake as significant (25). Furthermore, all changes in rest tumor volumes in ^{18}F-FET PET below 2 cm^3 were considered as insignificant and set to zero for statistical evaluation (patients 8, 13, and 25) because the calculation of $T_{vol\ 1.6}$ of ^{18}F-FET uptake in small residual tumor volumes is considerably influenced by partial-volume effects.

Statistics

Survival analysis was performed using Kaplan–Meier estimates for PFS and OS (data are presented as median values). The log-rank test was used for global comparison of PFS and OS curves between the subgroups. As general prognostic factors, the RPA score, extent of resection, MGMT status, and $T_{vol\ 1.6}$ in FET-1 at a cutoff of 25 cm^3 were considered (Table 2) (14). To evaluate the prognostic impact of treatment-related variations in PET and MRI,

TABLE 3
Prognostic Impact of Changes of TBR$_{max}$, TBR$_{mean}$, T$_{vol\ 1.6}$, and Gd-Volume on Survival

Change	FET/MRI-2 vs. FET/MRI-1 — PFS (mo)				OS (mo)				FET/MRI-3 vs. FET/MRI-1 — PFS (mo)				OS (mo)			
	P	Hazard ratio	95% CI	Value	P	Hazard ratio	95% CI	Value	P	Hazard ratio	95% CI	Value	P	HR	95% CI	Value
^{18}F-FET TBR$_{max}$	0.002*	0.206	0.069–0.612		<0.001*	0.155	0.047–0.505		0.14	0.502	0.198–1.273		0.02*	0.259	0.092–0.733	
Responder change ≤ −10%				9.3 (n = 17)				15.4 (n = 17)				8.3 (n = 17)				15.4 (n = 17)
Nonresponder change > −10%				4.7 (n = 6)				8.5 (n = 6)				5.2 (n = 7)				9.3 (n = 7)
^{18}F-FET TBR$_{mean}$	<0.001*	0.156	0.051–0.480		<0.001*	0.123	0.036–0.415		0.76	0.937	0.408–2.155		0.54	0.759	0.329–1.750	
Responder change ≤ −5%				10.3 (n = 14)				16.1 (n = 14)				7.2 (n = 11)				16.1 (n = 11)
Nonresponder change > −5%				5.1 (n = 9)				9.3 (n = 9)				8.3 (n = 13)				14.3 (n = 13)
^{18}F-FET T$_{vol\ 1.6}$	0.04*	0.346	0.133–0.994		0.39	0.772	0.323–1.894		0.002*	0.259	0.103–0.655		0.06	0.529	0.231–1.211	
Responder change ≤ 0%				9.3 (n = 15)				14.8 (n = 15)				9.4 (n = 15)				16.1 (n = 15)
Nonresponder change > 0%				5.8 (n = 8)				9.8 (n = 8)				5.1 (n = 9)				9.9 (n = 9)
MRI Gd-volume	0.65	1.059	0.413–2.711		0.83	1.049	0.416–2.650		0.23	0.501	0.197–1.271		0.38	0.706	0.288–1.731	
Responder change ≤ 0%				6.6 (n = 14)				14.3 (n = 14)				10.3 (n = 10)				14.8 (n = 10)
Nonresponder change > 0%				8.3 (n = 7)				16.1 (n = 7)				7.2 (n = 11)				14.3 (n = 11)

*Significant.
HR = hazard ratio; CI = confidence interval.

the changes of TBR_{max}, TBR_{mean}, and $T_{vol\ 1.6}$ in ^{18}F-FET PET and Gd-volume in MRI were tested. A P value of 0.05 or less was considered statistically significant. The data of the statistical tests are corrected for multiple statistical testing using the Bonferroni adjustment. The results of the statistical tests are given without correction for multiple statistical testing. It is explicitly noted, however, if the significance level was greater than 0.05 after performing a Bonferroni correction.

A multivariate Cox regression analysis was performed for the changes of each TBR_{max}, TBR_{mean}, and $T_{vol\ 1.6}$ in ^{18}F-FET PET, and Gd-volume in MRI in relation to RPA score, prescribed radiation dose, MGMT status, postoperative $T_{vol\ 1.6}$ (FET-1), and extent of resection to investigate which of these variables constitutes an independent prognostic factor with respect to PFS and OS. This analysis was done for each parameter separately. Hazard rate ratios and their 95% confidence intervals were calculated (Table 4). All statistical tests to which they apply were 2-sided.

ROC curves were drawn for the changes of TBR_{max}, TBR_{mean}, and $T_{vol\ 1.6}$ in ^{18}F-FET PET and Gd-volume in MRI, and the areas under the curves (AUC) were calculated. For a specific parameter, the cutoff level that resulted in the highest product of sensitivity and specificity was considered the optimal cutoff for prognostication.

Statistical analysis was performed using SigmaStat software (for Windows 11.0; SigmaPlot) and PASW statistics software (Release 18.0.3; SPSS Inc.).

RESULTS

Patient Data

The median follow-up was 13.8 mo (range, 3–29 mo). The clinical data of the patients and the results of TBR_{max}, TBR_{mean}, and $T_{vol\ 1.6}$ in ^{18}F-FET PET and Gd-volumes in MRI are presented in Table 1. The statistical influence of general prognostic factors is shown in Table 2.

Survival According to General Prognostic Factors

The mean PFS and OS of all patients ($n = 25$) were 9.2 mo (median, 7.2 mo; range, 2.8–28.7 mo) and 14.1 mo (median, 13.8 mo; range, 2.8–28.7 mo). Well-established prognostic factors such as the RPA score and extent of tumor resection showed a trend toward significance on PFS and OS. For the MGMT status and postoperative $T_{vol\ 1.6}$ in FET-1 less than 25 cm³, respectively, a significantly longer PFS and OS could be observed (Table 2). In our patient group, neither radiation technique (3-dimensional radiation treatment vs. intensity-modulated radiotherapy)

nor prescribed radiation dose had a significant influence on prognosis.

Survival According to Gd-Volume

The relationship of survival and treatment-related changes of the Gd-volume between MRI-1 and MRI-2, and between MRI-1 and MRI-3, was tested at cutoff values of ≤0% vs. >0% and ≤−25% vs. >−25% (Tables 3 and 4; Supplemental Table 4). Testing of further cutoff values led to strong disparity of group sizes and was discarded. No significant differences of PFS and OS between the different groups could be detected. ROC analysis yielded no significant results.

Survival According to Changes of TBR_{max} and TBR_{mean} of ^{18}F-FET Uptake

Using the approximation procedure, the best discriminative power to separate the patients in 2 prognostic groups was identified at a decrease of the TBR_{max} of more than 10% (≤−10% vs. >−10%) (Table 3). Testing of further cutoff values led to strong disparity of group sizes (Supplemental Table 2). Early metabolic ^{18}F-FET PET responders with a decrease of the TBR_{max} between FET-1 and FET-2 (≤−10%) had a significantly longer median PFS (9.3 vs. 4.7 mo; $P = 0.002$) and OS (15.4 vs. 8.5 mo; $P < 0.001$) than nonresponders (Table 3). ROC analysis confirmed also the best cut point for TBR_{max} to predict PFS at −10%. For prediction of OS, the optimal cut point of TBR_{max} was slightly different (−20%), as may be explained by statistical effects due to the small size of the group. According to ROC analysis, a decrease of the TBR_{max} between FET-1 and FET-2 of more than 20% allowed the identification of patients with OS less than median, with a sensitivity of 83% and a specificity of 67% (AUC, 0.75; $P = 0.04$; Supplemental Table 1). Also, the follow-up at FET-3 showed a longer OS for metabolic responders than for nonresponders (15.4 vs. 9.3 mo; $P = 0.02$); however, this difference is not significant after Bonferroni adjustment.

For TBR_{mean}, similar results were obtained. The best discriminative power was identified at a decrease of TBR_{mean} more than 5% (≤−5% vs. >−5%) using the approximation procedure (Table 3). With a trend toward significance, the same cut point was determined by ROC

TABLE 4
Multivariate Analysis (Cox Proportional Hazards Model) of Imaging-Related Factors vs. RPA Score, Prescribed Radiation Dose, MGMT Status, Postoperative $T_{vol\ 1.6}$ (FET-1), and Extent of Resection

Variable	Analysis of PFS			Analysis of OS		
	P	Hazard ratio	95% confidence interval	P	Hazard ratio	95% confidence interval
TBR_{max} (FET-2 vs. FET-1)	0.017*	0.122	0.021–0.691	0.028*	0.197	0.046–0.841
TBR_{mean} (FET-2 vs. FET-1)	0.035*	0.216	0.052–0.899	0.05*	0.195	0.037–1.029
$T_{vol\ 1.6}$ (FET-3 vs. FET-1)	0.007*	0.142	0.034–0.588	0.07	0.326	0.097–1.094
Gd-volume (MRI-3 vs. MRI-1)	0.311	0.558	0.181–1.724	0.197	0.447	0.131–1.518

*Significant.

analysis to predict PFS and OS. The decrease of the TBR_{mean} between FET-1 and FET-2 allowed the identification of patients with PFS and OS less than median with a sensitivity of 67% and a specificity of 75% (AUC, 0.72; $P = 0.08$ and 0.07, respectively; Supplemental Table 1). Again, early metabolic responders with a decrease of the TBR_{mean} between FET-1 and FET-2 ($\leq -5\%$) exhibited a significantly longer median PFS (10.3 vs. 5.1 mo) and OS (16.1 vs. 9.3 mo) ($P < 0.001$ for both PFS and OS; Table 3). The varying of thresholds ($\leq 0\%$ vs. $> 0\%$ and $\leq -10\%$ vs. $> -10\%$) showed results with poorer discrimination power (Supplemental Table 2).

Multivariate Cox regression analysis confirmed early changes of TBR_{max} and TBR_{mean} (FET-2 vs. FET-1) as significant independent predictors of PFS and OS (Table 4). The Kaplan–Meier plots of PFS and OS of early metabolic responders and nonresponders according to the TBR_{mean} of ^{18}F-FET uptake ($\leq -5\%$ vs. $> -5\%$) are shown in Figure 1.

Survival According to Changes of $T_{vol\ 1.6}$

To evaluate the prognostic influence of changes of the tumor volume in ^{18}F-FET PET, patients were separated into a group of metabolic responders who showed a stable or decreasing $T_{vol\ 1.6}$ in ^{18}F-FET PET (relative change $\leq 0\%$) and a group of nonresponders who showed an increasing $T_{vol\ 1.6}$ in ^{18}F-FET PET (relative change $> 0\%$) (Table 3; Supplemental Table 3). Separating the groups at other cutoff values led to a strong disparity of group sizes and was discarded. Early after completion of RCX (FET-2), the met-

abolic responders with stable or reduced tumor volume in ^{18}F-FET PET had a weakly significantly longer PFS than the nonresponders (9.4 vs. 5.8 mo; $P = 0.04$; Table 3). However, after Bonferroni adjustment this observation was not significant. At 6–8 wk after completion of RCX (FET-3), however, changes of $T_{vol\ 1.6}$ in ^{18}F-FET PET had a more significant prognostic value, especially for PFS (9.3 vs. 5.1 mo; $P = 0.002$; Table 3). For OS, only a trend could be observed ($P = 0.06$). ROC analysis yielded no significant results.

Multivariate Cox regression analysis confirmed changes of $T_{vol\ 1.6}$ at further follow-up (FET-3 vs. FET-1) as an independent predictor of PFS (Table 4).
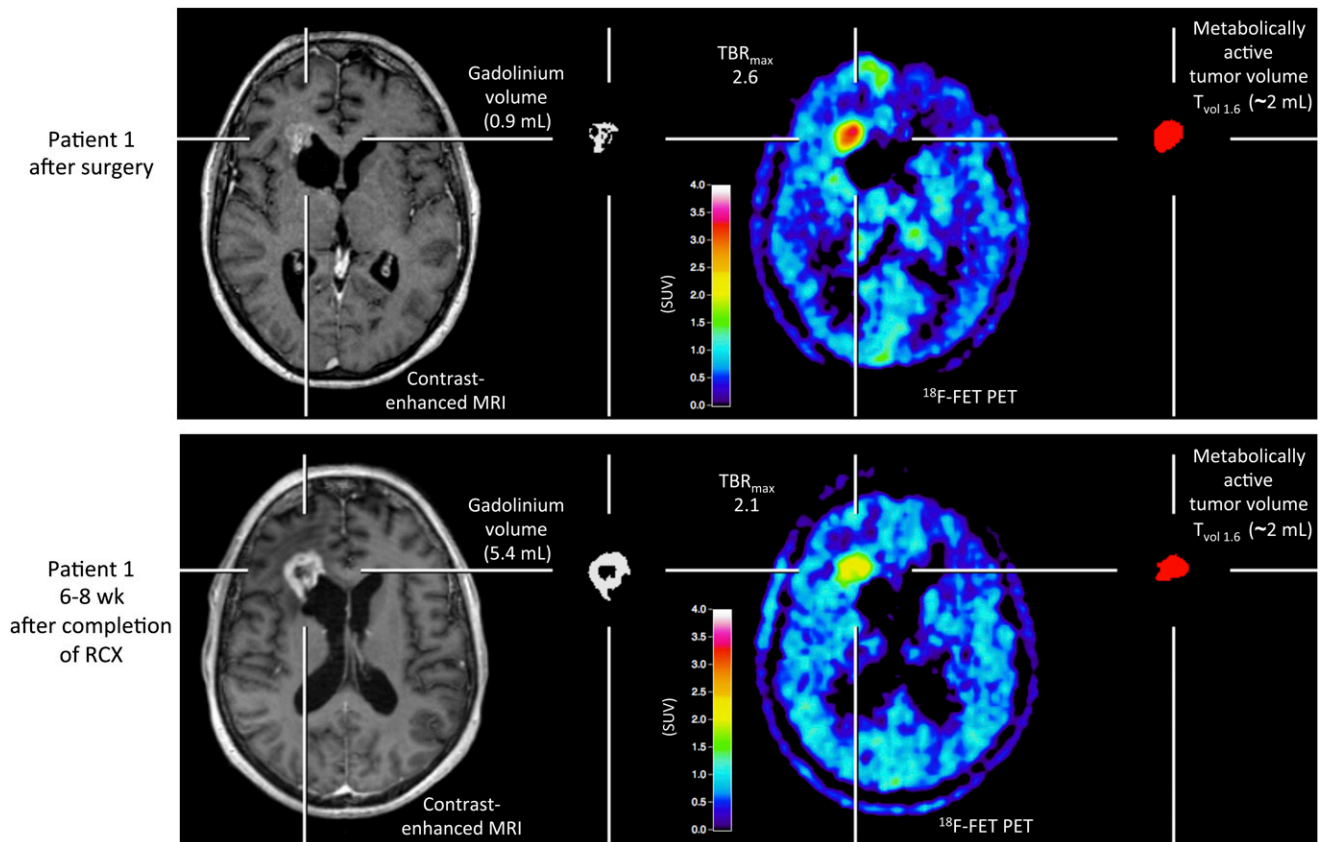
Pseudoprogression

Five of 25 patients (20%) had pseudoprogression on MRI (patients 1, 6, 16, 19, and 23; Fig. 2 shows images of patient 1). All these patients had a favorable median PFS and OS (9.3 and 16.1 mo, respectively). Furthermore, in patients with pseudoprogression the median reduction of TBR_{max} and TBR_{mean} was 22% and 11%, respectively, and the $T_{vol\ 1.6}$ remained stable (median change, 0%). In contrast, all patients showed an increase of the Gd-volume (median change, 433%).

DISCUSSION

The results of this prospective study suggest that the decrease of ^{18}F-FET accumulation as indicated by TBR_{mean} and TBR_{max} reflects the reaction of the tumor to the therapeutic intervention at an early stage of the disease (FET-2)
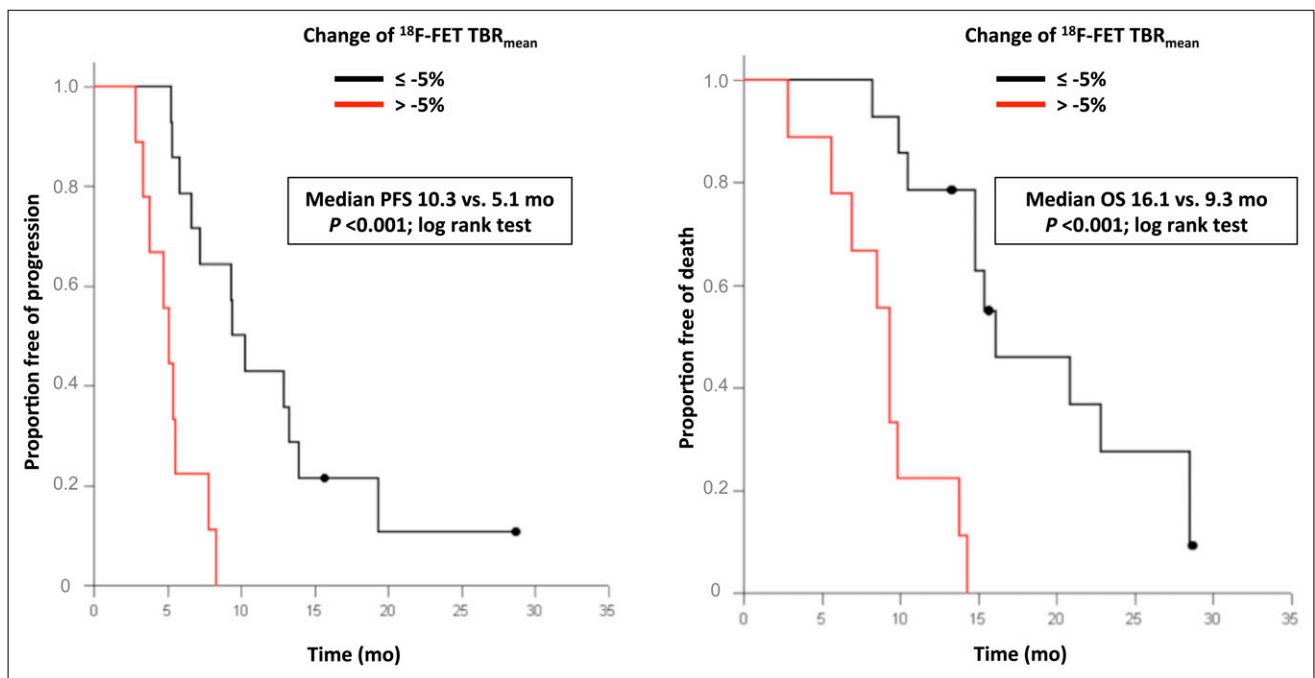
FIGURE 1. Kaplan–Meier curves of PFS (left) and OS (right) of patients with glioblastoma according to treatment-related changes of TBR_{mean} in ^{18}F-FET PET early after completion of RCX (FET-2 vs. FET-1). Metabolic responders with decrease of TBR_{mean} of more than 5% ($\leq -5\%$) show significantly longer PFS and OS than nonresponders. Censored observations are marked with dots.

FIGURE 2. Patient example of pseudoprogression (patient 1). Brain imaging after surgery (upper; MRI-/FET-1) and 6–8 wk after completion of radiochemotherapy (lower; MRI-/FET-3). Contrast-enhanced MRI with corresponding Gd-volume is shown on left and ^{18}F-FET PET with corresponding $T_{vol\ 1.6}$ on right. Enlargement of Gd-volume on MRI after 6- to 8-wk completion of RCX (lower) is suggesting tumor progression, whereas ^{18}F-FET PET indicates responder with decreasing amino acid uptake (reduction of TBR_{max}) and unchanged $T_{vol\ 1.6}$. Patient had favorable outcome, with PFS of 14.1 and OS of 16.1 mo.

and predicts outcome. At a later stage (FET-3), changes of the TBR in relation to baseline are less predictive, and changes of $T_{vol\ 1.6}$ may be of additional value. Therefore, the data indicate that various parameters derived from ^{18}F-FET PET may be useful to predict treatment response at an early stage of disease and may thereby help to optimize individual treatment. Moreover, especially the reduction of TBRs derived from ^{18}F-FET PET may add valuable additional information to diagnose pseudoprogression within 6–8 wk after RCX.

In contrast to the ^{18}F-FET PET results, in our study treatment-related changes of Gd-volumes in contrast-enhanced MRI failed to predict treatment response and showed no relationship with patient survival. Although the extent of MRI contrast enhancement in malignant gliomas is routinely used as an indicator of therapeutic response (26), this approach is limited by the difficulty in distinguishing between tumor and treatment-induced necrosis (27). Reliable prognostic information can be obtained only several months after the initiation of treatment. For several reasons, however, the ability to differentiate tumor progression from pseudoprogression is essential (Figs. 2 and 3). First, considerable morbidity is associated with unneces-

sary surgical interventions; second, because pseudoprogression spontaneously resolves, the ability to identify such lesions could prevent futile treatment from being given; and third, because chemotherapy is often adjusted after tumor progression (6).

The results of our study are in line with the observations of several studies that evaluated the role of amino acid PET using ^{11}C-methionine and ^{18}F-FET to monitor treatment effects in smaller groups of patients during a standard chemotherapy regimen—that is, adjuvant temozolomide (5/28) or procarbazine, lomustine (CCNU), and vincristine (PCV) chemotherapy (10,28); dose-intensified chemotherapy with temozolomide (29); and experimental treatment (e.g., intracavitary radioimmunotherapy, convection-enhanced delivery of paclitaxel, and tyrosine kinase inhibitor treatment) (12,13,30). Furthermore, the relevance of metabolically active tumor volumes in amino acid PET to assess treatment response is further supported by more recent studies (16,21,31,32).

Although conventional MRI cannot reliably distinguish between tumor and pseudoprogression, several alternative MRI techniques are presently evaluated that may overcome this problem (6,33). For example, diffusion and perfusion-
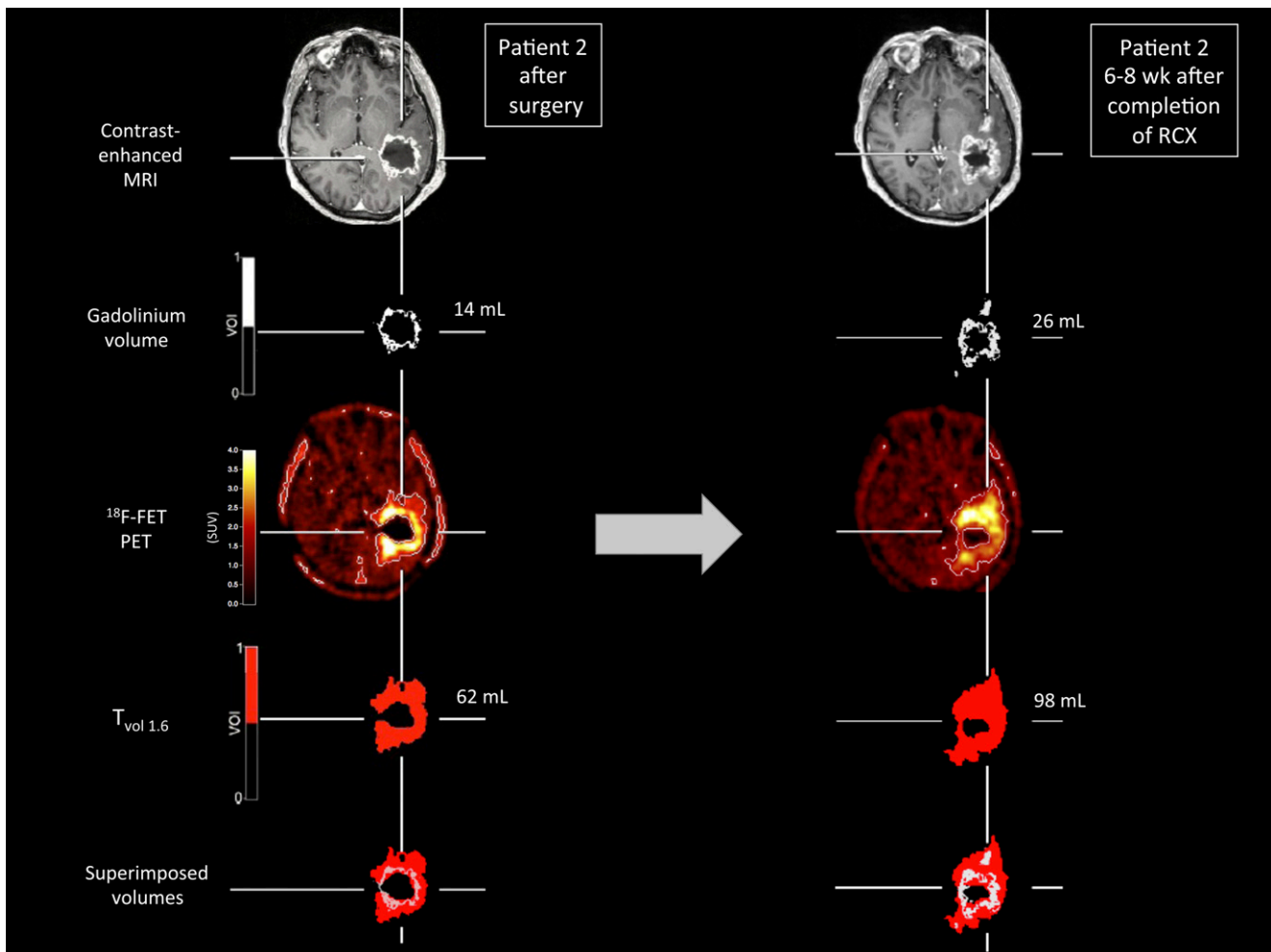
FIGURE 3. Patient example of nonresponder according to ¹⁸F-FET PET (patient 2). (Left) Imaging after surgery (FET-1/MRI-1). (Right) Imaging results 6–8 wk after completion of RCX (FET-3/MRI-3). Patient exhibits increasing ¹⁸F-FET uptake in course of disease (right). In comparison to imaging after surgery, coregistration of ¹⁸F-FET PET scan, contrast-enhanced MRI, and volumes of interest of contrast enhancement and $T_{vol\ 1.6}$ in transaxial orientation exhibit that metabolically active tumor volume is considerably larger than volume of contrast enhancement, has eccentric configuration, and covers entire contrast-enhancing volume (bottom). In this patient, PFS and OS were relatively short, at 8.3 and 9.3 mo, respectively.

weighted imaging have been considered (*34,35*), but the clinical relevance of these methods is not yet established (*6*). These developments are rather encouraging, and comparative studies are needed to investigate the relationship, diagnostic performance, and complementary character of amino acid PET and modern MRI techniques.

Some shortcomings of this study need to be discussed. Inasmuch as data on the reproducibility of the TBR of ¹⁸F-FET uptake in brain tumors are not yet available, experience with other tyrosine derivates had to be considered. With the tyrosine analog ¹²³I-iodo-α-methyltyrosine, a maximal deviation of the TBR of 5% has been observed in repeated studies, indicating that the TBR of amino acid uptake in brain tumors is a rather stable parameter (*25*). Furthermore, it cannot be excluded that the PET signal in the baseline scan may have been due to postoperative changes and not residual macroscopic tumor tissue. Although residual uptake of ¹⁸F-FET after surgery has not

yet been investigated histologically, ¹¹C-methionine uptake after repeated surgery of residual childhood brain tumors showed that increased tracer uptake corresponded well with vital tumor tissue (*36*). Because the results with ¹¹C-methionine and ¹⁸F-FET in brain tumors are similar (*37*), we assume unspecific ¹⁸F-FET uptake with a TBR of more than 1.6 in the postoperative phase is unlikely.

Finally, the patient number in this prospective study is small, and the results need to be considered with caution. Nevertheless, to the best of our knowledge, there is to date no larger prospective study in the literature concerning this topic.

CONCLUSION

The results of this study suggest that therapeutically induced changes in ¹⁸F-FET PET may be a useful measure to predict treatment response at an early stage of disease and may thereby help to optimize individual treatment. In

contrast to Gd-volumes on MRI, changes in ^{18}F-FET PET may be a valuable parameter to assess treatment response in glioblastoma and to predict survival time. Further studies are needed to investigate the clinical role of modern approaches of MRI in combination with amino acid PET to solve this important clinical issue.

DISCLOSURE STATEMENT

ACKNOWLEDGMENT

REFERENCES

1. Laws ER, Parney IF, Huang W, et al. Survival following surgery and prognostic factors for recently diagnosed malignant glioma: data from the Glioma Outcomes Project. *J Neurosurg.* 2003;99:467–473.
2. Stupp R, Mason WP, van den Bent MJ, et al. Radiotherapy plus concomitant and adjuvant temozolomide for glioblastoma. *N Engl J Med.* 2005;352:987–996.
3. DeAngelis LM. Brain tumors. *N Engl J Med.* 2001;344:114–123.
4. Kumar AJ, Leeds NE, Fuller GN, et al. Malignant gliomas: MR imaging spectrum of radiation therapy- and chemotherapy-induced necrosis of the brain after treatment. *Radiology.* 2000;217:377–384.
5. Wen PY, Macdonald DR, Reardon DA, et al. Updated response assessment criteria for high-grade gliomas: response assessment in neuro-oncology working group. *J Clin Oncol.* 2010;28:1963–1972.
6. Yang I, Aghi MK. New advances that enable identification of glioblastoma recurrence. *Nat Rev Clin Oncol.* 2009;6:648–657.
7. Jager PL, Vaalburg W, Pruim J, de Vries EG, Langen KJ, Piers DA. Radiolabeled amino acids: basic aspects and clinical applications in oncology. *J Nucl Med.* 2001;42:432–445.
8. Pauleit D, Floeth F, Hamacher K, et al. O-(2-[18F]fluoroethyl)-L-tyrosine PET combined with MRI improves the diagnostic assessment of cerebral gliomas. *Brain.* 2005;128:678–687.
9. Pöpperl G, Götz C, Rachinger W, Gildehaus FJ, Tonn JC, Tatsch K. Value of O-(2-[18F]fluoroethyl)-L-tyrosine PET for the diagnosis of recurrent glioma. *Eur J Nucl Med Mol Imaging.* 2004;31:1464–1470.
10. Galldiks N, Kracht LW, Burghaus L, et al. Use of ^{11}C-methionine PET to monitor the effects of temozolomide chemotherapy in malignant gliomas. *Eur J Nucl Med Mol Imaging.* 2006;33:516–524.
11. Ribom D, Eriksson A, Hartman M, et al. Positron emission tomography ^{11}C-methionine and survival in patients with low-grade gliomas. *Cancer.* 2001;92:1541–1549.
12. Pöpperl G, Götz C, Rachinger W, et al. Serial O-(2-[18F]fluoroethyl)-L: -tyrosine PET for monitoring the effects of intracavitary radioimmunotherapy in patients with malignant glioma. *Eur J Nucl Med Mol Imaging.* 2006;33:792–800.
13. Pöpperl G, Goldbrunner R, Gildehaus FJ, et al. O-(2-[18F]fluoroethyl)-L-tyrosine PET for monitoring the effects of convection-enhanced delivery of paclitaxel in patients with recurrent glioblastoma. *Eur J Nucl Med Mol Imaging.* 2005;32:1018–1025.
14. Piroth MD, Holy R, Pinkawa M, et al. Prognostic impact of postoperative, pre-irradiation ^{18}F-fluoroethyl-l-tyrosine uptake in glioblastoma patients treated with radiochemotherapy. *Radiother Oncol.* 2011;99:218–224.
15. Thiele F, Ehmer J, Piroth MD, et al. The quantification of dynamic FET PET imaging and correlation with the clinical outcome in patients with glioblastoma. *Phys Med Biol.* 2009;54:5525–5539.
16. Hutterer M, Nowosielski M, Putzer D, et al. O-(2-[18F-fluoroethyl)-L-tyrosine PET predicts failure of antiangiogenic treatment in patients with recurrent high-grade glioma. *J Nucl Med.* 2011;52:856–864.
17. Piroth MD, Pinkawa M, Holy R, et al. Prognostic value of early [18F]fluoroethyl-tyrosine positron emission tomography after radiochemotherapy in glioblastoma multiforme. *Int J Radiat Oncol Biol Phys.* 2011;80:176–184.
18. Curran WJ Jr, Scott CB, Horton J, et al. Recursive partitioning analysis of prognostic factors in three Radiation Therapy Oncology Group malignant glioma trials. *J Natl Cancer Inst.* 1993;85:704–710.
19. Hegi ME, Diserens AC, Gorlia T, et al. MGMT gene silencing and benefit from temozolomide in glioblastoma. *N Engl J Med.* 2005;352:997–1003.
20. International Commission on Radiation Units and Measurements (ICRU). *Prescribing, Recording and Reporting Photon Beam Therapy (Report 50).* Bethesda, MD: ICRU; 1993. Available at: http://www.icru.org/index.php?option=com_content&task=view&id=72. Accessed May 10, 2012.
21. Galldiks N, Ullrich R, Schroeter M, Fink GR, Jacobs AH, Kracht LW. Volumetry of [11C]-methionine PET uptake and MRI contrast enhancement in patients with recurrent glioblastoma multiforme. *Eur J Nucl Med Mol Imaging.* 2010;37:84–92.
22. Vollmar S, Hampl J, Kracht L, Herholz K. Integration of functional data (PET) into brain surgery planning und neuronavigation. *Springer Proceedings in Physics.* 2007;114:98–103.
23. Hamacher K, Coenen HH. Efficient routine production of the ^{18}F-labelled amino acid O-2-^{18}F fluoroethyl-L-tyrosine. *Appl Radiat Isot.* 2002;57:853–856.
24. Macdonald DR, Cascino TL, Schold SC Jr, Cairncross JG. Response criteria for phase II studies of supratentorial malignant glioma. *J Clin Oncol.* 1990;8:1277–1280.
25. Langen KJ, Roosen N, Coenen HH, et al. Brain and brain tumor uptake of L-3-[123I]iodo-alpha-methyl tyrosine: competition with natural L-amino acids. *J Nucl Med.* 1991;32:1225–1229.
26. Grant R, Liang BC, Slattery J, Greenberg HS, Junck L. Chemotherapy response criteria in malignant glioma. *Neurology.* 1997;48:1336–1340.
27. Levivier M, Becerra A, De Witte O, Brotchi J, Goldman S. Radiation necrosis or recurrence. *J Neurosurg.* 1996;84:148–149.
28. Herholz K, Kracht LW, Heiss WD. Monitoring the effect of chemotherapy in a mixed glioma by C-11-methionine PET. *J Neuroimaging.* 2003;13:269–271.
29. Galldiks N, Kracht LW, Burghaus L, et al. Patient-tailored, imaging-guided, long-term temozolomide chemotherapy in patients with glioblastoma. *Mol Imaging.* 2010;9:40–46.
30. Galldiks N, Ullrich R, Schroeter M, Fink GR, Kracht LW. Imaging biological activity of a glioblastoma treated with an individual patient-tailored, experimental therapy regimen. *J Neurooncol.* 2009;93:425–430.
31. Wyss M, Hofer S, Bruehlmeier M, et al. Early metabolic responses in temozolomide treated low-grade glioma patients. *J Neurooncol.* 2009;95:87–93.
32. Chen W, Geist C, Czernin J, et al. Assess treatment response using FDOPA PET in patients with recurrent malignant gliomas treated with bevacizumab and irinotecan [abstract]. *J Nucl Med.* 2008;49(suppl 1):78P.
33. Dhermain FG, Hau P, Lanfermann H, Jacobs AH, van den Bent MJ. Advanced MRI and PET imaging for assessment of treatment response in patients with gliomas. *Lancet Neurol.* 2010;9:906–920.
34. Bobek-Billewicz B, Stasik-Pres G, Majchrzak H, Zarudzki L. Differentiation between brain tumor recurrence and radiation injury using perfusion, diffusion-weighted imaging and MR spectroscopy. *Folia Neuropathol.* 2010;48:81–92.
35. Tsien C, Galban CJ, Chenevert TL, et al. Parametric response map as an imaging biomarker to distinguish progression from pseudoprogression in high-grade glioma. *J Clin Oncol.* 2010;28:2293–2299.
36. Pirotte B, Goldman S, Van Bogaert P, et al. Integration of [11C]methionine-positron emission tomographic and magnetic resonance imaging for image-guided surgical resection of infiltrative low-grade brain tumors in children. *Neurosurgery.* 2005;57:128–139.
37. Grosu AL, Astner ST, Riedel E, et al. An interindividual comparison of O-(2-[18F]fluoroethyl)-L-tyrosine (FET)- and L-[methyl-11C]methionine (MET)-PET in patients with brain gliomas and metastases. *Int J Radiat Oncol Biol Phys.* 2011;81:1049–1058.